# Development of SD Field with Storm-Time at Kakioka

By Yukio Yokouchi


## 概　　要

柿岡にて観測された磁気嵐資料により *SD* field の時間的推移を調査した.


## § 1. Introduction

In the previous paper [1] the results of statistical studies for *Dst*-variations and *SD*-variations of the first and second days after the commencements of magnetic storms with sudden commencement by the data observed at Kakioka ($\lambda$ : 140° 11′ E, $\varphi$ : 36° 14′ N, $\varphi_m$ : 26°.0) were reported for the period 1924～1951. On the other-hand, it was desired to have a thorough knowledge of development of *SD*-field with storm-time. On this problem, the data at Sitka and the data at the world wide distributed stations including Kakioka were analyzed statistically by Dr. T. Nagata & H. Ono [2] in 1952, and recently by Dr. M. Sugiura & S. Chapman [3], respectively. Although in this paper the data at Kakioka are also analyzed statistically for development of *SD*-field with storm-time, it is expected to give more detail knowledge for Kakioka's data. In the previous paper geomagnetic storms with sudden commencements (*ssc*) are classified in three groups SC(a), SC(b) and SC(c), and so here, the data of groups SC(a) (123 storms), SC(c) (143 storms) and SC(a) + SC(c) (266 storms) are used for the investigation.

## § 2. Harmonic amplitude and phase of *SD*-variations of successive intervals of each 24 hours

The average *SD*-variations for the first day after the commencement of storm obtained in the previous paper are illustrated in Fig. 1 with vector arrow representation of the overhead electric equivalent current responsible to the horizontal force disturbance.

First, the *SD*-variations for 24 hours are calculated for the following intervals of storm-time, (0～23), (1～24)……(24～47) and (25～48) hour, and their harmonic amplitudes and phases of the diurnal component are shown in Fig. 2. The amplitude $c_n$ and phase angle $\varphi_n$ of the Fourier series are given by $\sum_n c_n \sin(nt+\varphi_n)$ or $\sum_n a_n \cos nt + b_n \sin nt$, where $t$ is reckoned from the 135°E. M. midnight. In this paper,

1′ in D corresponds to 8.7γ in H·△D and D is positive if toward the East and Z is positive if downward. It seems that the mean *SD*-variations for interval of 24 hours give reliable data, because there are normalized or excluded the errors that may introduce from differences of the intensities of storms, ground levels of storms and magnetic history on pre-day of the commencement of storm. It will be seen from the figure that the amplitude of *SD*-variation of H for SC(a) shows a maximum at intervals (0~23)~(2~25) hour and then decreases gradually, while for SC(c) a maximum at around interval (18~41) hour. The phase angles of *SD*-variations are kept nearly constant throughout the whole period of storm-time within the range of 15°~30°.

## § 3. Storm-local time diagram and analysis of *SD*-variation for different storm-time

Since the results mentioned above are obtained from the mean *SD*-variations for interval 24 hours, they are scarcely representative in detail with regard to the development of *SD* with storm-time. In this paper is used the method of so-called storm-time diagram after Dr. Nagata & Ono [2] for the investigation of the development of *SD*-field. Namely, the hourly values of H-, D- and Z- traces the period from 0 hour to 48 hour after the commencements of storms are subtracted by the quiet daily mean variations of corresponding months, and grouped for storms occurred at different local times, averaging for each storm-time to get eventually 24 series consisting of 49 hourly values. In this case, the obtained values are measured from the pre-storm levels deduced from the 24 hours mean values before commencements. As shown in Fig. 3~5, these hourly values are written on a storm-local time diagram according to their storm- and local-times and contour-lines are mapped. Moreover, from the values of this diagram the *SD*-variations for different storm-times are obtained. As the geomagnetic latitude $\varphi_m$ of Kakioka is 26°.0 and *SD* is not expected to be so predominant and numbers of data are not so numerous, it seems that there are some irreguralities in the present results. In Fig. 3~5 are shown storm-local time diagrams, where it is obvious that the mean variation of columns shows the mean *Dst* and the mean variations of abscissas for storm-times 0~23 and 24~47 hour show the mean *SD*s of the first and second days of storms, respectively.

In Fig. 6 are shown the harmonic amplitudes and phases for the *SD*-variations for different storm-times. As for the diurnal component, SC(a) in H shows the greater amplitudes at about storm-times 8~18 hour which is the similar tendency with the results of T. Nagata [2] and S. Sugiura [3], but in the present result

duration of greater values is longer. On the other-hand, it is noted that for SC(c) in H the change of amplitudes is greatly different from that of SC(a) with a maximum at about storm-time 38 hour. These results are related to those shown in Fig. 2. The phase of the diurnal component is nearly constant with small change in the first about 24 hours, but thereafter changes in larger extent, especially in H for SC(a). It seems that various errors appear more predominant as the amplitudes become smaller. The amplitudes of the semi-diurnal component are comparable to those of the diurnal component, showing roughly similar tendencies in changes. In Fig. 7, it is seen that in H the phase angles of the semi-diurnal component decrease 30° every one hour of storm-time for both SC(a) and SC(c), and they are 300° at storm-time 0 hour. In D and Z there is no such a rather remarkable regular change, but remains a roughly similar tendency with some irregularities.

In Fig. 8~12 are shown harmonic dials for inspection of more detail. For the *SD*-variations of the first and second days in H, D and Z, ratios of the semi-diurnal component to the diurnal component are in the range 0.1~0.5, mean 0.3 and hence this shows that the amplitude of the semi-diurnal component for interval 24 hours diminishes according to the above mentioned fact of decrease of 30° every storm-time 1 hour by averaging over a whole day.

Now, the cause of this fact is considered roughly as follows. For the first time, differences of ground levels of storms can not be checked in the present data, but it is not likely to expect exactly the same circumstance for SC(a) and SC(c). Next, it seems to be most appropriate to examine whether there is a distribution of intensity of storms responsible for the cause of this fact, or not. Here, the maximum ranges in H for storms are used tentatively as an index of intensity of storm and in Fig. 13 are shown the hourly distribution of the ranges to mean ones. The smoothed curve of ratio for SC(a) are $0.2 \sin(2t+63°)$ for the semi-diurnal component. This shows that there are two maxima at 1 and 13 hour and two minima at 7 and 19 hour in local time. If it is assumed that this change obtained is effective to the phase on the semi-diurnal component of *SD*, the phase of this curve is 297° (−63°) at storm-time 0 hour, because values of H may be negatively larger as increasing intensity of storms. This value of 297° almost equals to 300° of phase angle of the semi-diurnal component of *SD*. On the other-hand, for SC(c) there is no such change but it seems that maximum ranges for SC(c) may not change proportionally to the intensity of storm, because storms of SC(c) are not alike with SC(a), but irregular in variations. We can not conclude here about this fact, but it is expected to investigate also by the data of other stations.

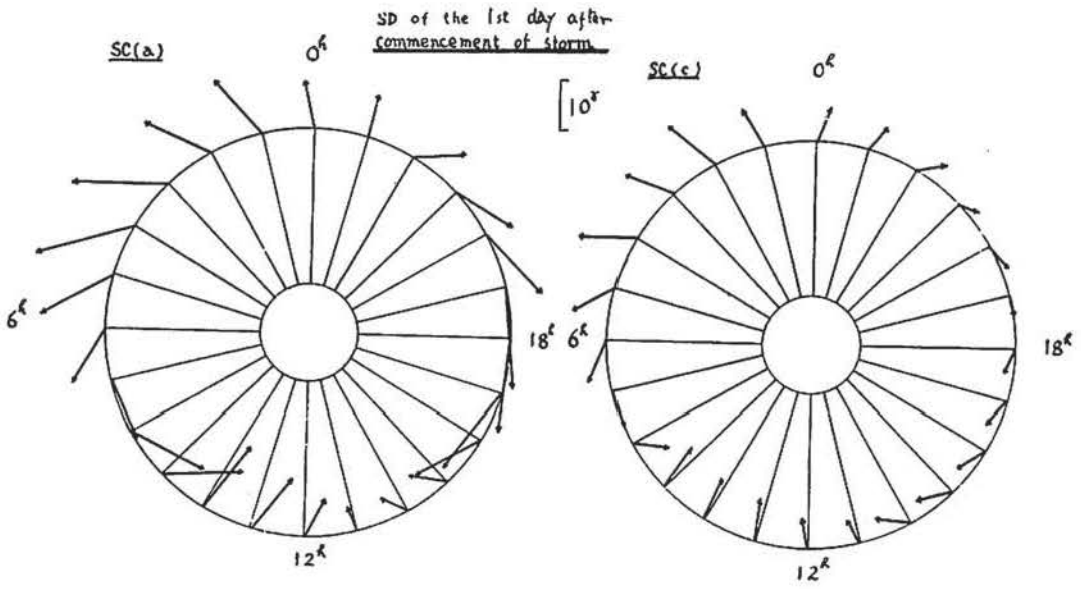


Fig. 1. Current vector diagram of average horizontal disturbing force of *SD* of first day after commencement of storm.

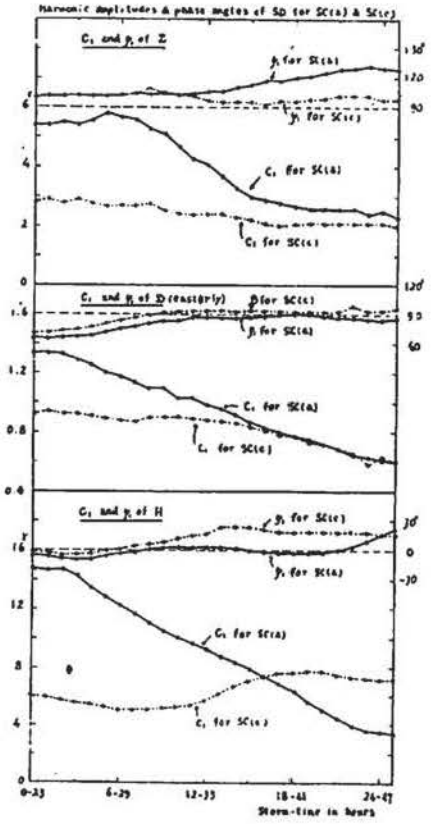


Fig. 2. Change with intervals of 24 hours of storm-time, (1–23), (2–24)……and (25–48) hour of amplitude and phase of diurnal component of *SD* of *ssc* in H, D and Z for storm groups SC(a) and SC(c) at Kakioka.

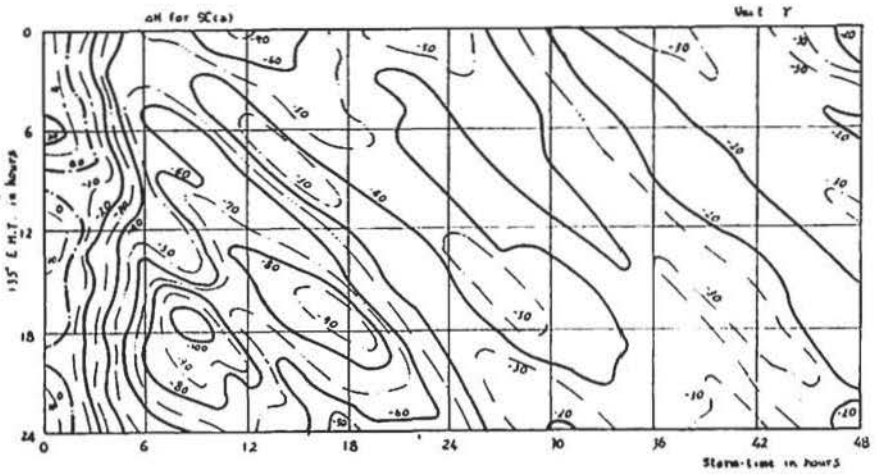


Fig. 3a. Storm–local time diagram of *Dst* and *SD* of *ssc* in H for storm group SC(a) at Kakioka.

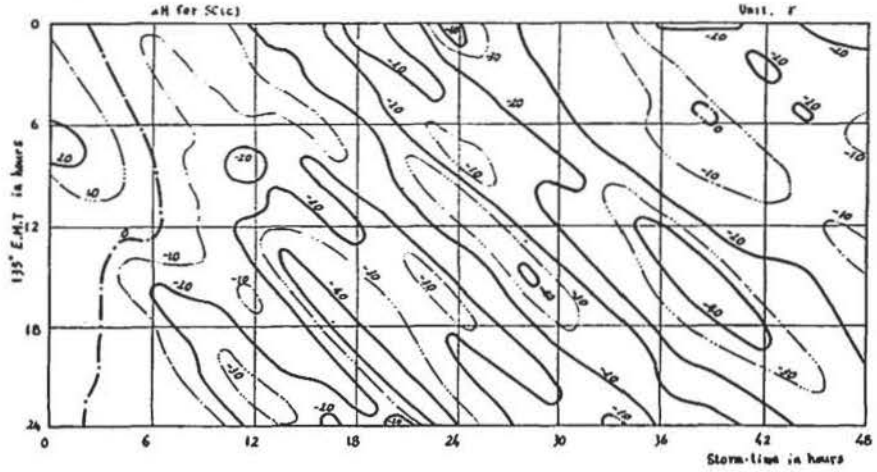


Fig. 3b. Storm–local time diagram of *Dst* and *SD* of *ssc* in H for storm group SC(c) at Kakioka.

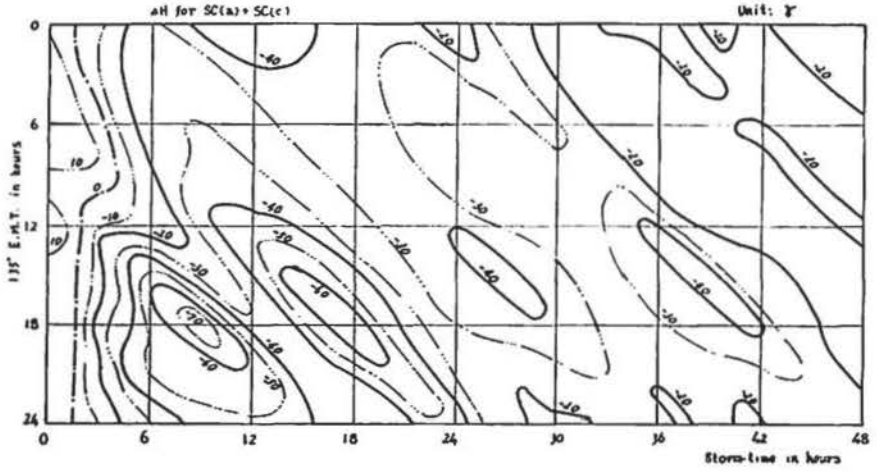


Fig. 3c. Storm–local time diagram of *Dst* and *SD* of *ssc* in H for storm group SC(a) +SC(c) at Kakioka.

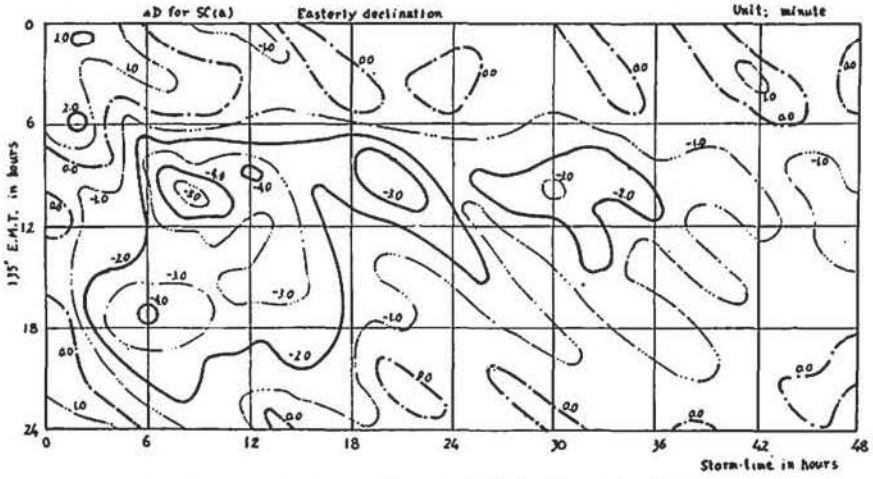


Fig. 4a. Storm-local time diagram of *Dst* and *SD* of *ssc* in D for storm group SC(a) at Kakioka.

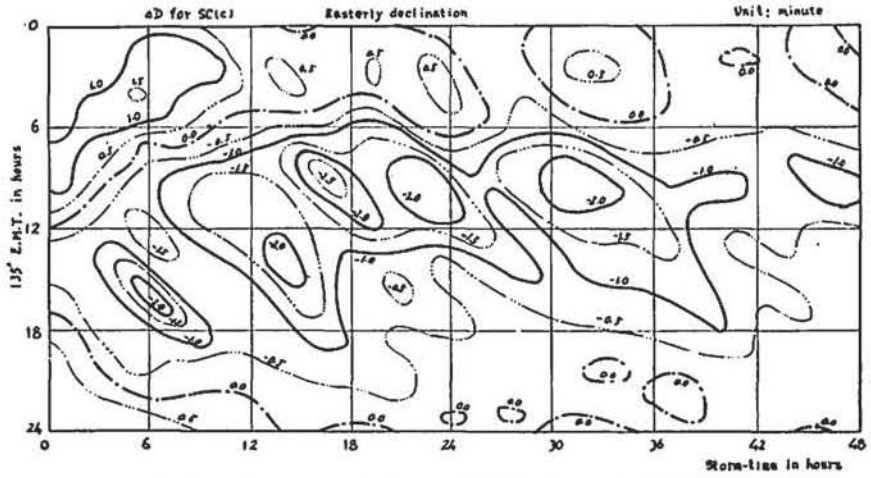


Fig. 4b. Storm-local time diagram of *Dst* and *SD* of *ssc* in D for storm group SC(c) at Kakioka.

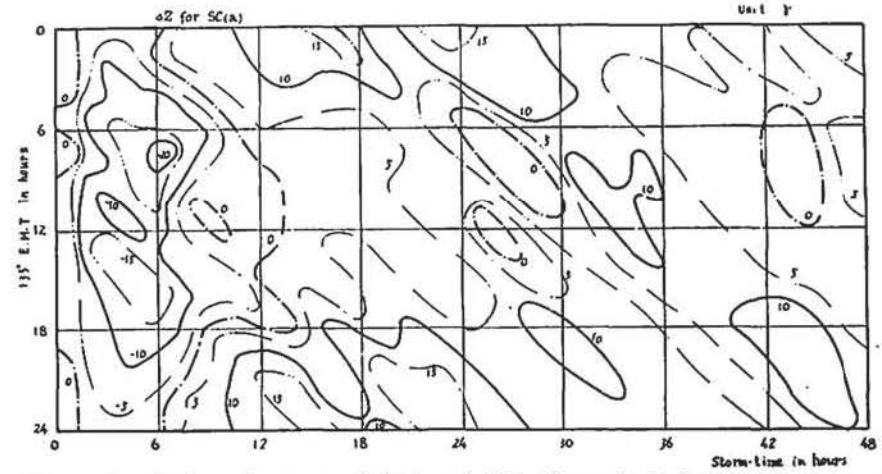


Fig. 5a. Storm-local time diagram of *Dst* and *SD* of *ssc* in Z for storm group SC(a) at Kakioka.

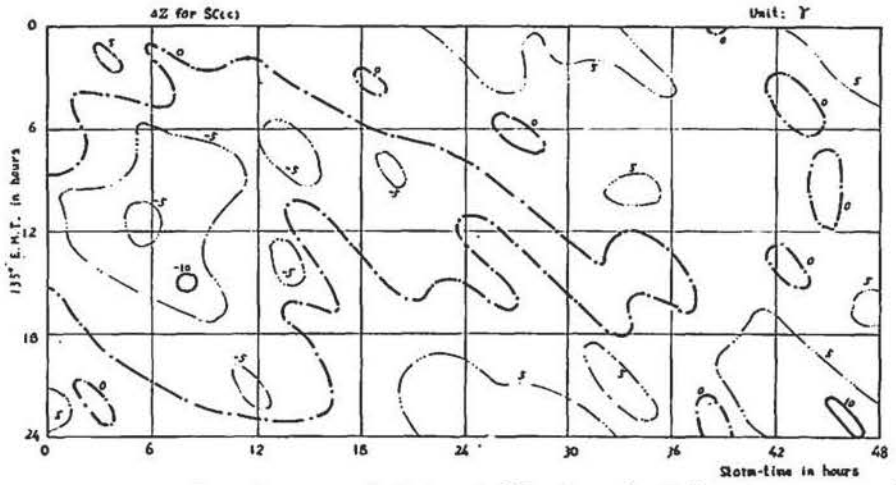


Fig. 5b. Storm-local time diagram of *Dst* and *SD* of *ssc* in Z for storm group SC(c) at Kakioka.

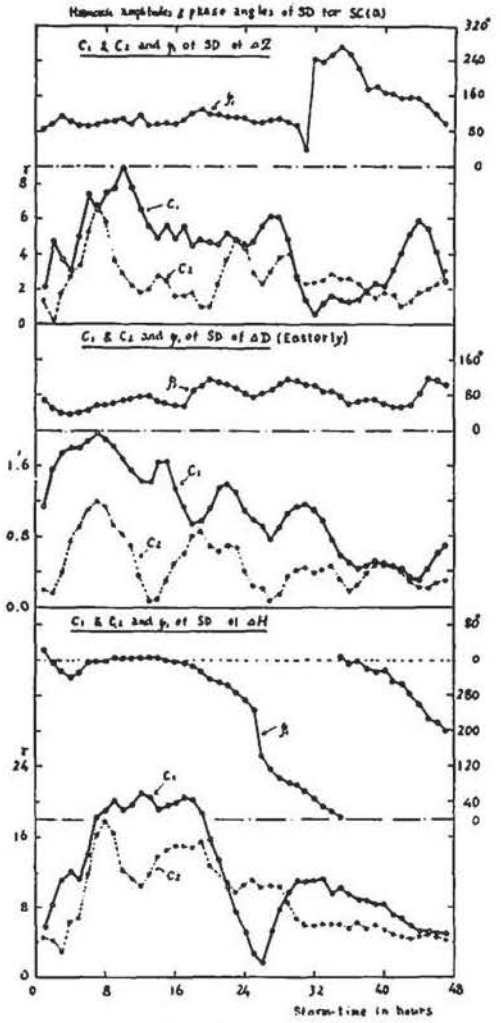


Fig. 6a. Change with storm-time of amplitude and phase of diurnal component and amplitude of semi-diurnal component of *SD* of *ssc* in H, D and Z for storm group SC(a) at Kakioka.

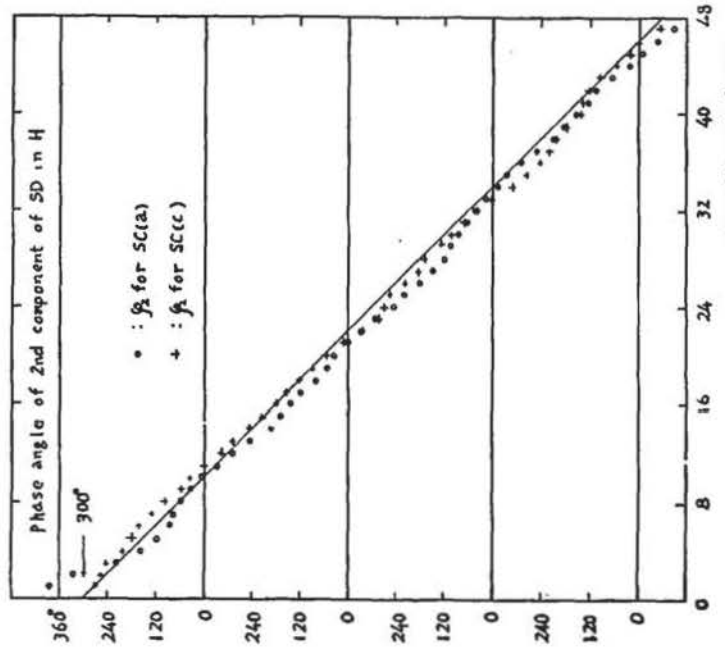


Fig. 7. Change with storm-time of phase angle of semi-diurnal component of *SD* of *ssc* in H for storm groups SC(a) and SC(c) at Kakioka.

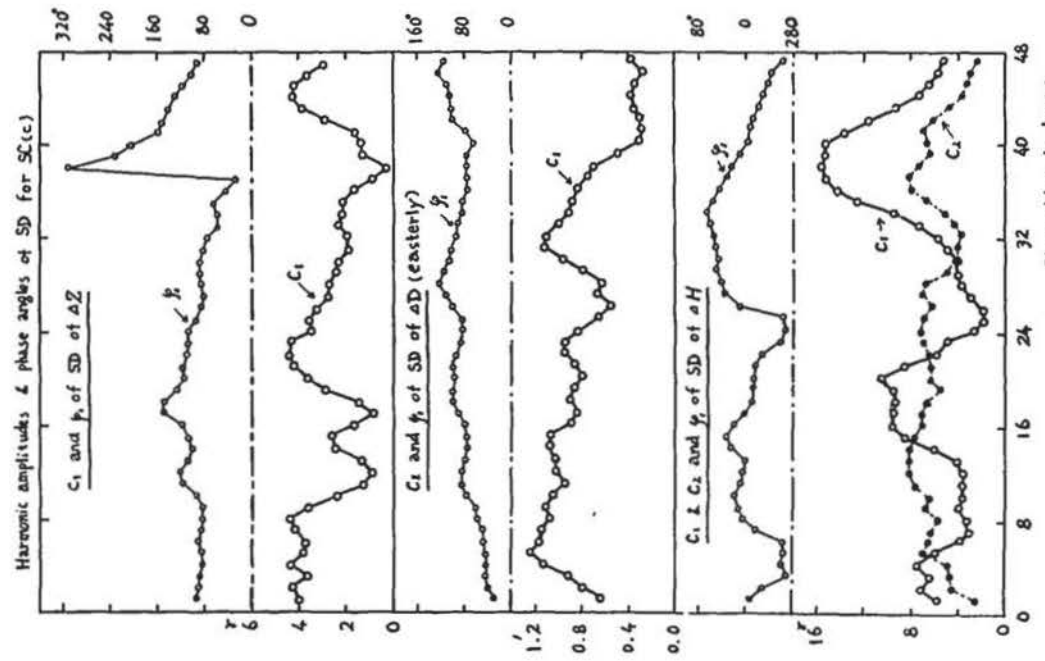


Fig. 6b. Change with storm-time of amplitude and phase of diurnal component and amplitude of semi-diurnal component of *SD* of *ssc* in H, D and Z for storm group SC(c) at Kakioka.

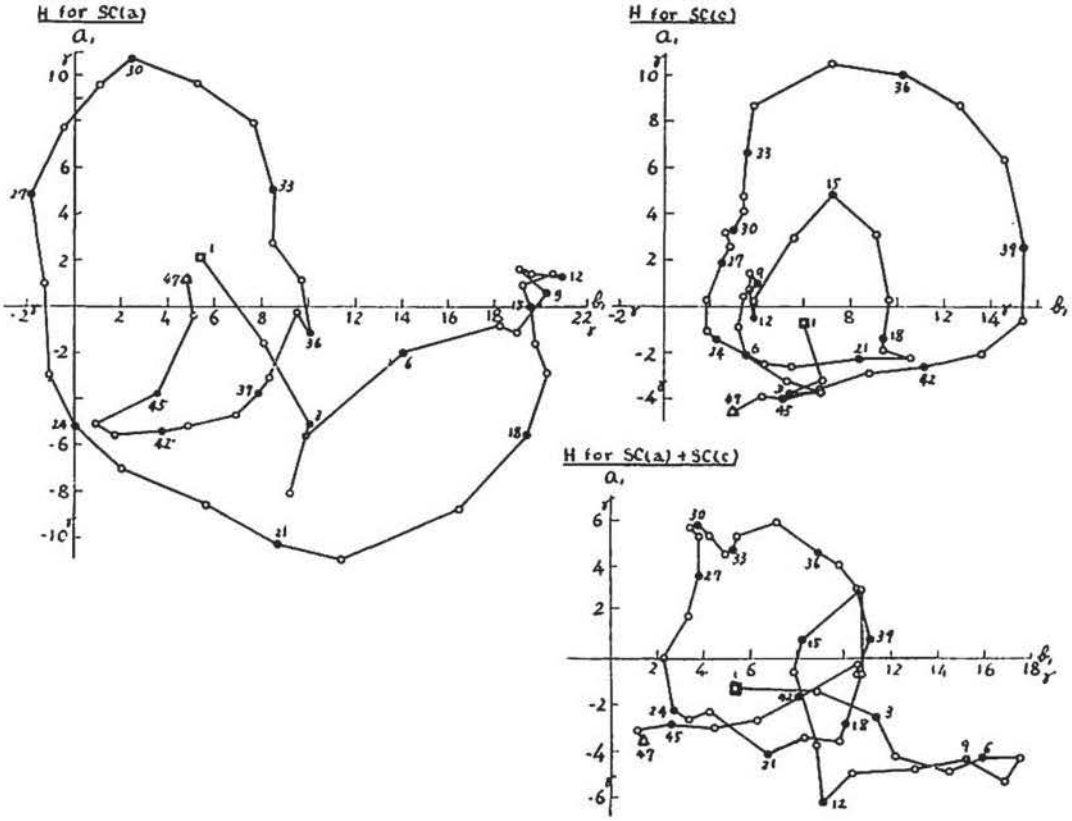


Fig. 8. Harmonic dials for diurnal component of *SD* in H for storm groups SC(a), SC(c) and SC(a)+SC(c) : 47 points refer to storm-time 1–47 hour.

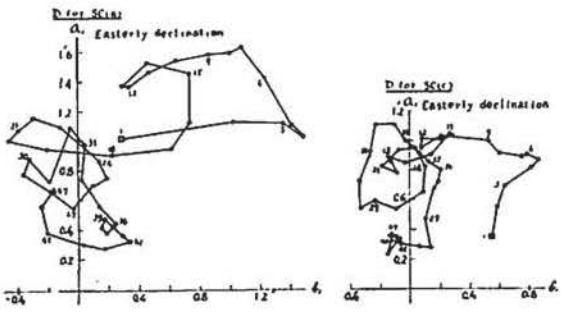

Fig. 9. Harmonic dials for diurnal component of *SD* in D for storm groups SC(a) and SC(c) : 47 points refer to storm-time 1–47 hour.

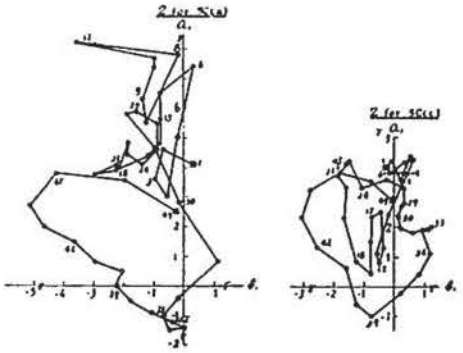

Fig. 10. Harmonic dials for diurnal component of *SD* in Z for storm groups SC(a) and SC(c) : 47 points refer to storm-time 1–47 hour.

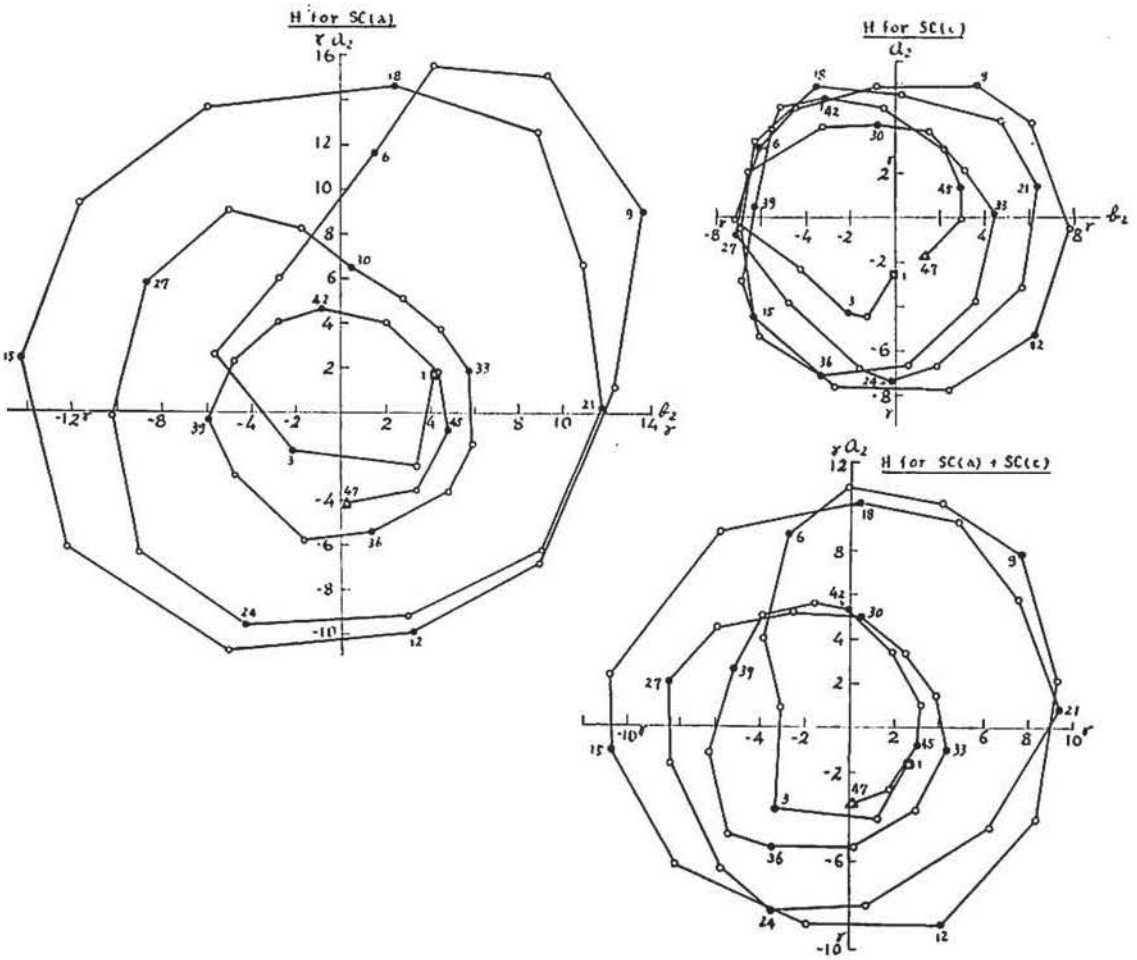


Fig. 11. Harmonic dials for semi-diurnal component of *SD* in H for storm groups SC(a), SC(c) and SC(a)+SC(c) : 47 points refer to storm-time 1–47 hour.

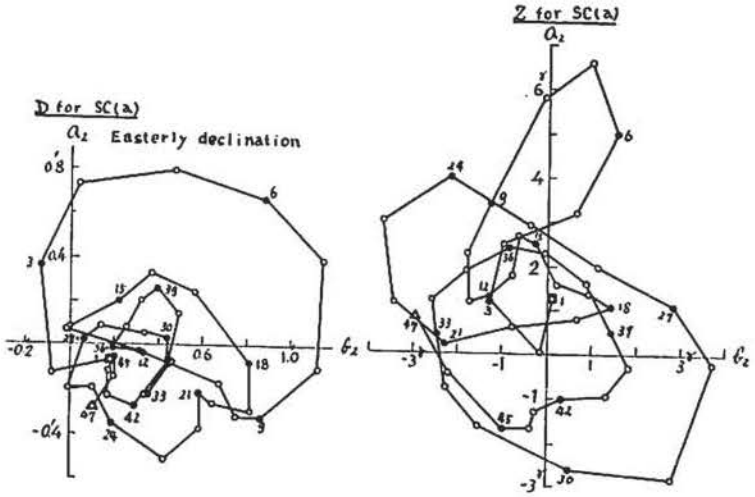


Fig. 12. Harmonic dials for semi-diurnal component of *SD* in D and Z for storm group SC(a) : 47 points refer to storm-time 1–47 hour.

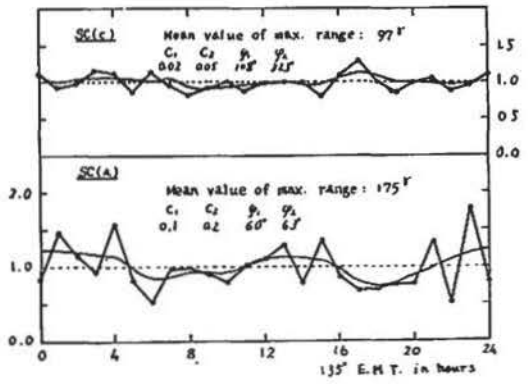


Fig. 13. Ratios of mean maximum ranges of *ssc* commenced at different local times to their total mean value.

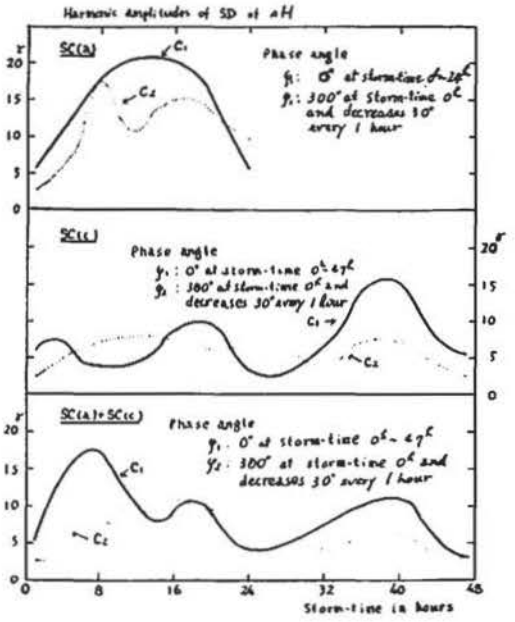


Fig. 14a. Change with storm-time of diurnal and semi-diurnal components of *SD* in H at Kakioka (smoothed value).

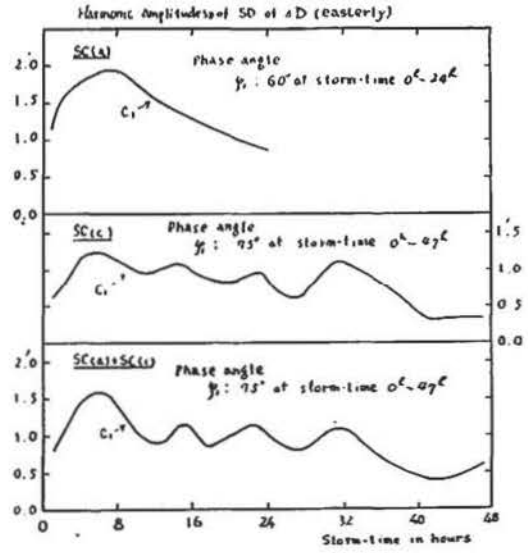


Fig. 14b. Change with storm-time of diurnal component of *SD* in D at Kakioka (smoothed value).

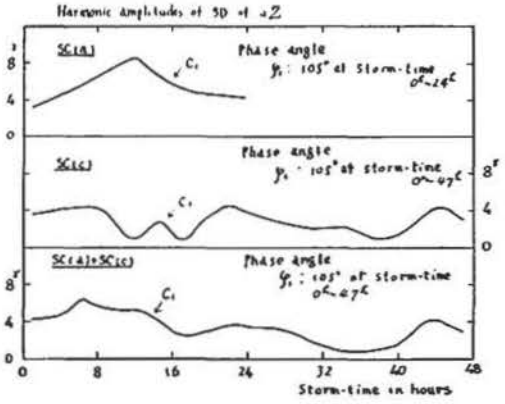


Fig. 14c. Change with storm-time of diurnal component of *SD* in Z at Kakioka (smoothed value).

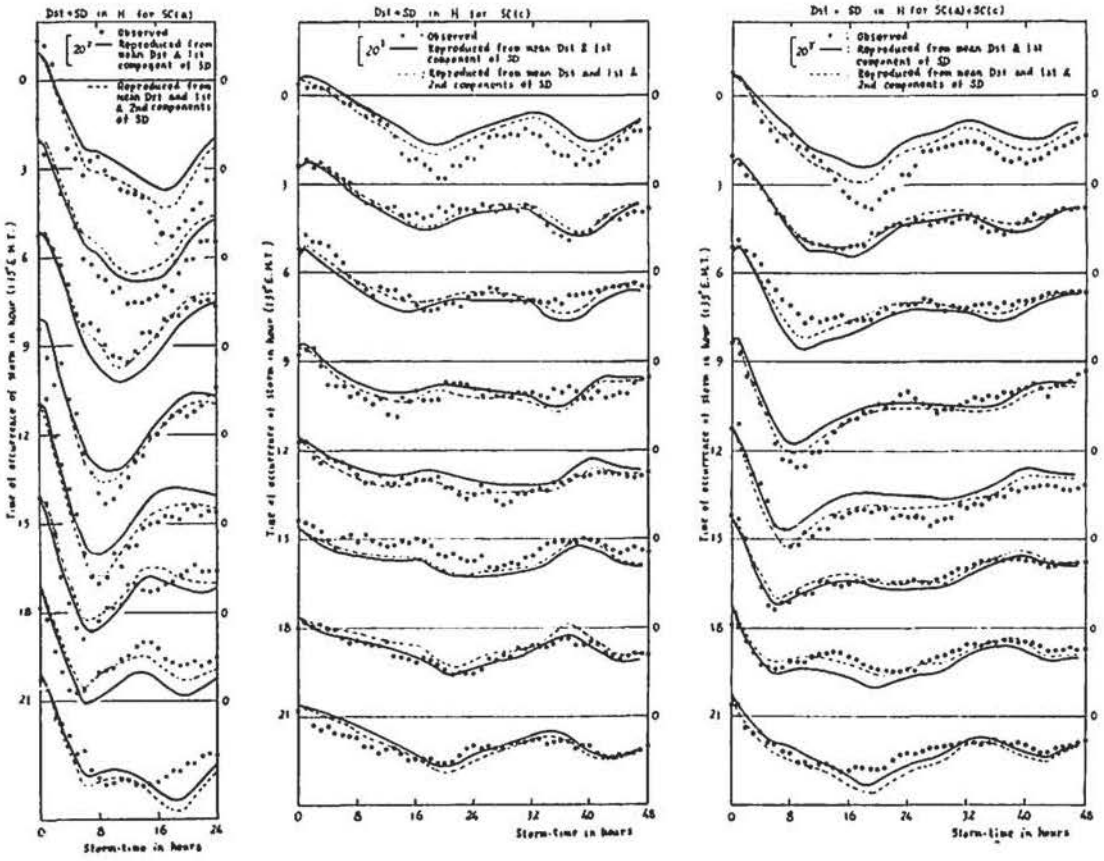

Fig. 15a. *Dst*+*SD* of *ssc* commenced at different local times in H for storm group SC(a) at Kakioka (observed and reproduced).

Fig. 15b. *Dst*+*SD* of *ssc* commenced at different local times in H for storm group SC(c) at Kakioka (observed and reproduced).

Fig. 15c. *Dst*+*SD* of *ssc* commenced at different local times in H for storm group SC(a) +SC(c) at Kakioka (observed and reproduced).

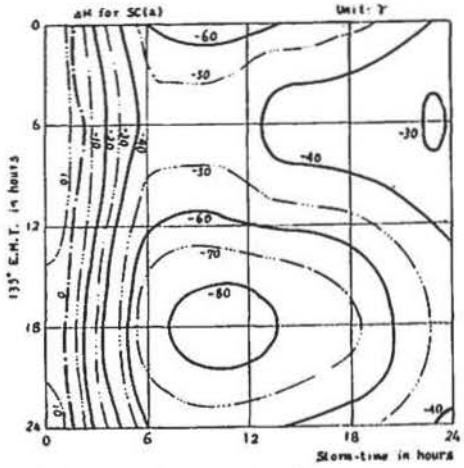


Fig. 16a. Storm–local time diagram of *Dst* and *SD* of *ssc* in H for storm group SC(a) (reproduced from mean *Dst* and diurnal component of *SD*).

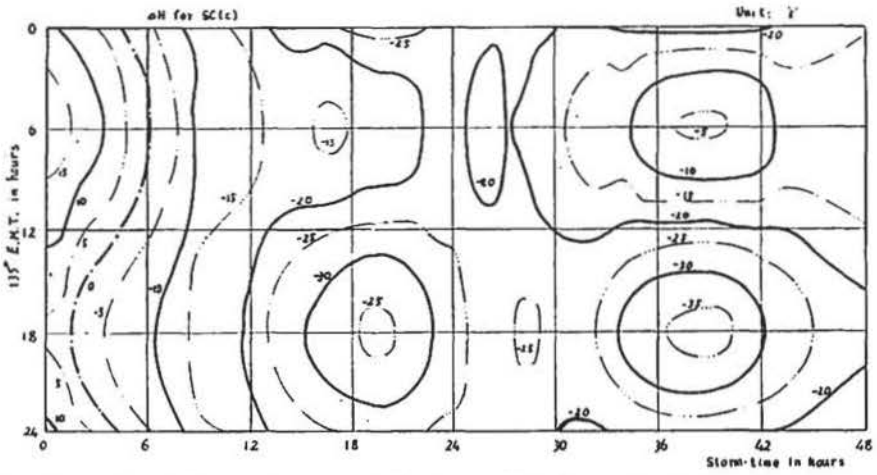


Fig. 16b. Storm–local time diagram of *Dst* and *SD* of *ssc* in H for storm group SC(c) (reproduced from mean *Dst* and diurnal component of *SD*).

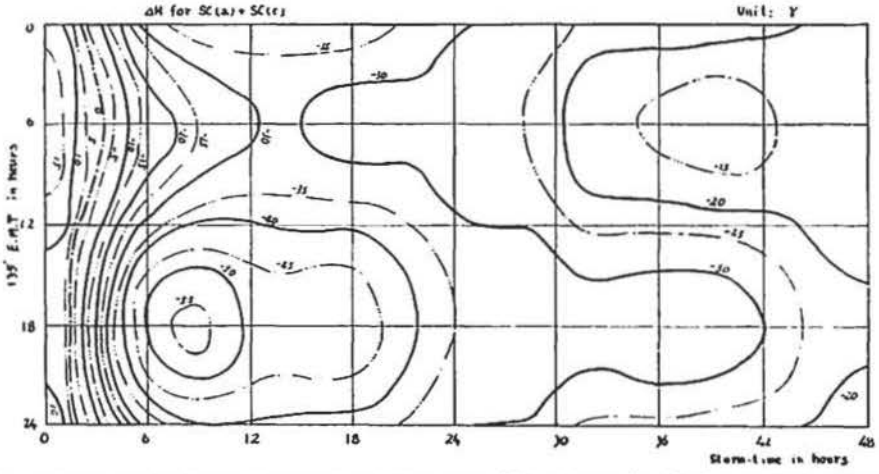


Fig. 16c. Storm–local time diagram of *Dst* and *SD* of *ssc* in H for storm group SC(a) + SC(c) (reproduced from mean *Dst* and diurnal component of *SD*).

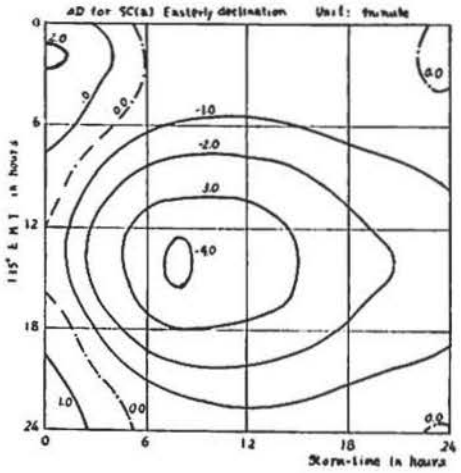


Fig. 17a. Storm–local time diagram of *Dst* and *SD* of *ssc* in D for storm group SC(a) (reproduced from mean *Dst* and diurnal component of *SD*).

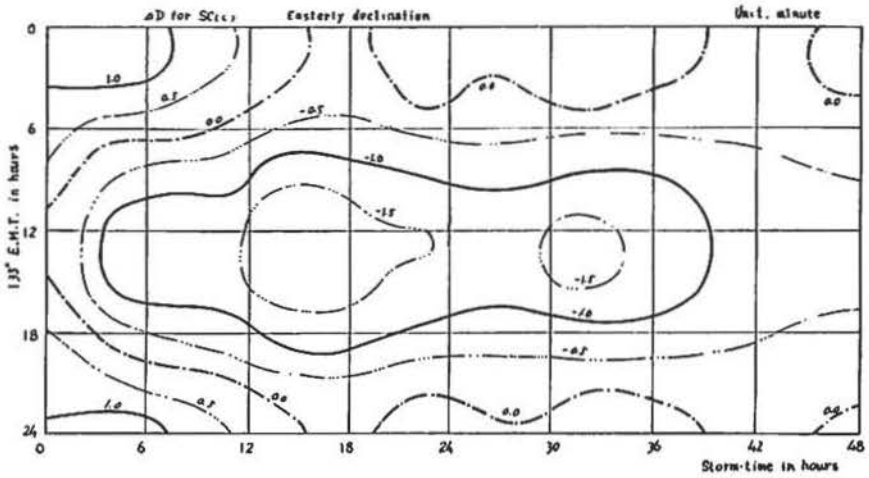


Fig. 17b. Storm–local time diagram of *Dst* and *SD* of *ssc* in D for storm group SC(c) (reproduced from mean *Dst* and diurnal component of *SD*).

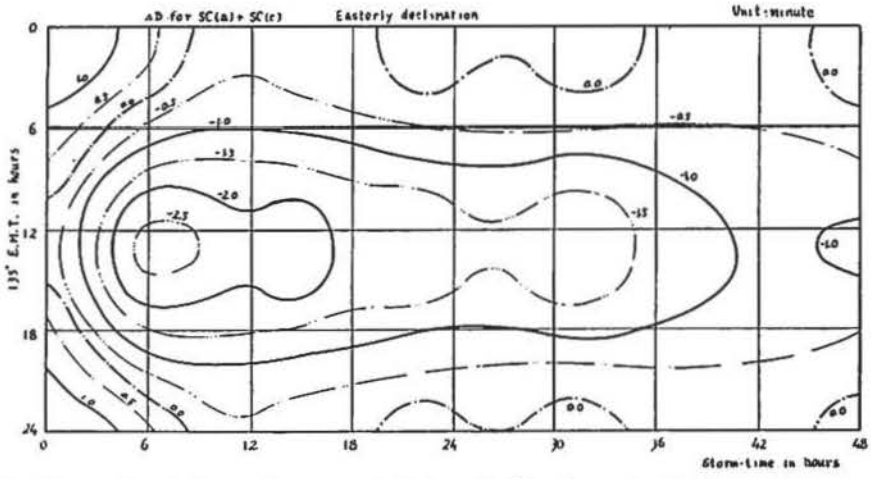


Fig. 17c. Storm–local time diagram of *Dst* and *SD* of *ssc* in D for storm group SC(a) + SC(c) (reproduced from mean *Dst* and diurnal component of *SD*).

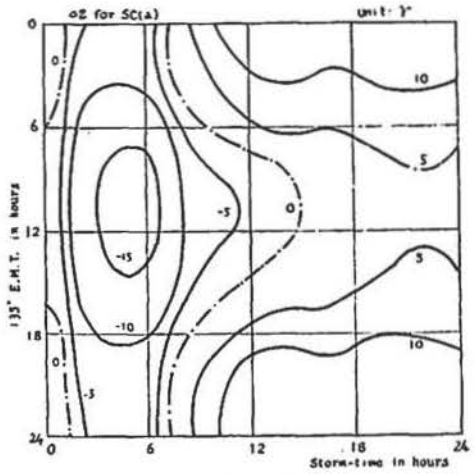


Fig. 18a. Storm–local time diagram of *Dst* and *SD* of *ssc* in Z for storm group SC(a) (reproduced from mean *Dst* and diurnal component of *SD*).

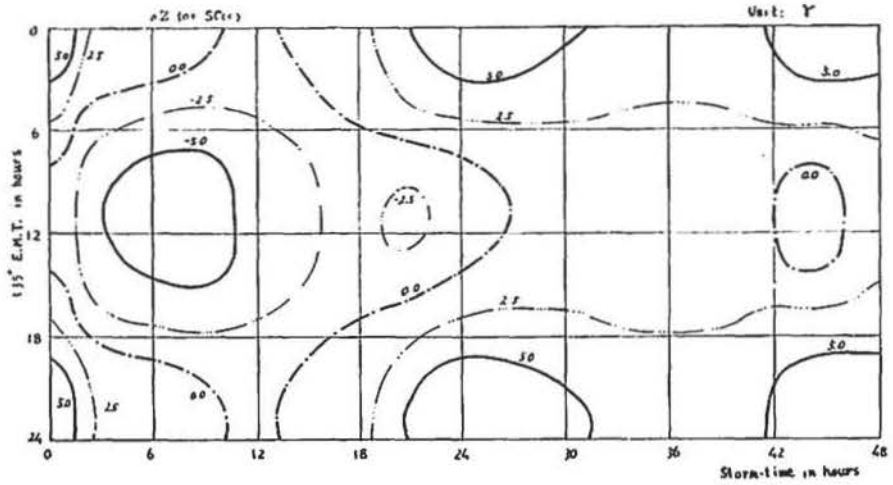


Fig. 18b. Storm–local time diagram of *Dst* and *SD* of *ssc* in Z for storm group SC(c) (reproduced from mean *Dst* and diurnal component of *SD*).

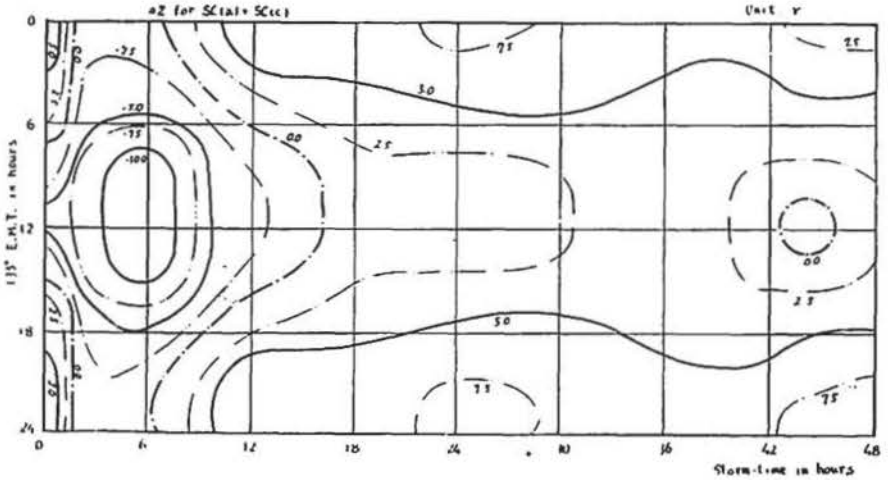


Fig. 18c. Storm–local time diagram of *Dst* and *SD* of *ssc* in Z for storm group SC(a) + SC(c) (reproduced from mean *Dst* and diurnal component of *SD*).

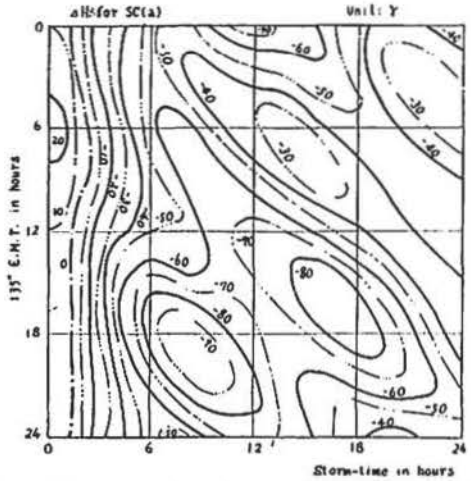


Fig. 19a. Storm–local time diagram of *Dst* and *SD* of *ssc* in H for storm group SC(a) (reproduced from mean *Dst* and diurnal and semi–diurnal components of *SD*).

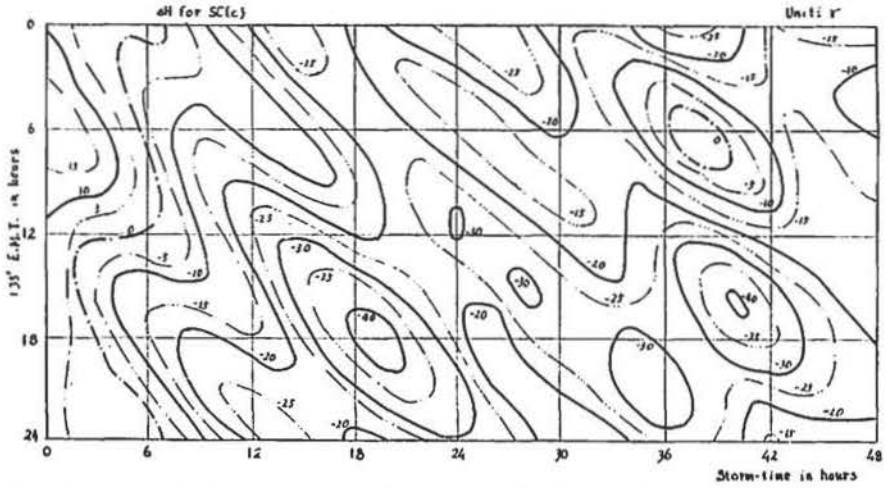


Fig. 19b. Storm–local time diagram of *Dst* and *SD* of *ssc* in H for storm group SC(c) (reproduced from mean *Dst* and diurnal and semi–diurnal components of *SD*).

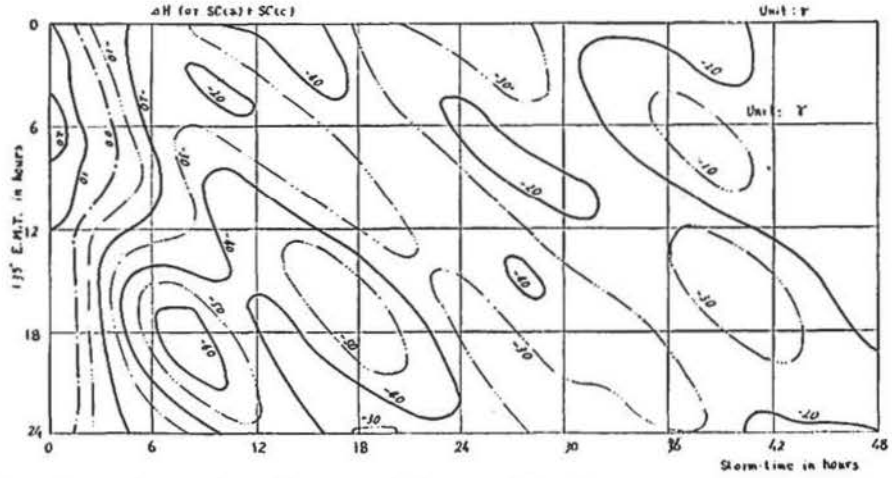


Fig. 19c. Storm–local time diagram of *Dst* and *SD* of *ssc* in H for storm group SC(a) +SC(c) (reproduced from mean *Dst* and diurnal and semi–diurnal components of *SD*).

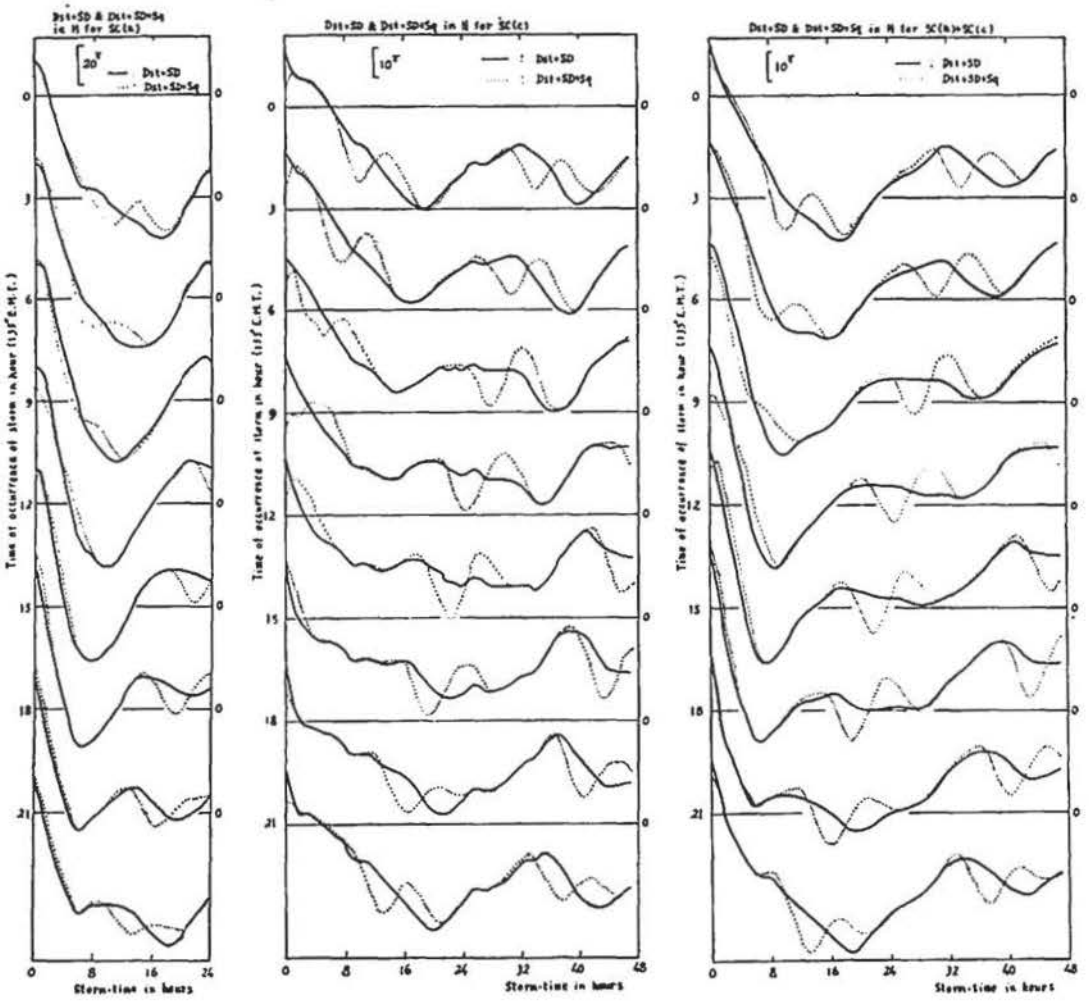

Fig. 20a. *Dst*+*SD* and *Dst*+*SD*+*Sq* of *ssc* commenced at different local times in H for storm group SC(a).

Fig. 20b. *Dst*+*SD* and *Dst*+*SD*+*Sq* of *ssc* commenced at different local times in H for storm group SC(c).

Fig. 20c. *Dst*+*SD* and *Dst*+*SD*+*Sq* of *ssc* commenced at different local times in H for storm group SC(a)+SC(c).

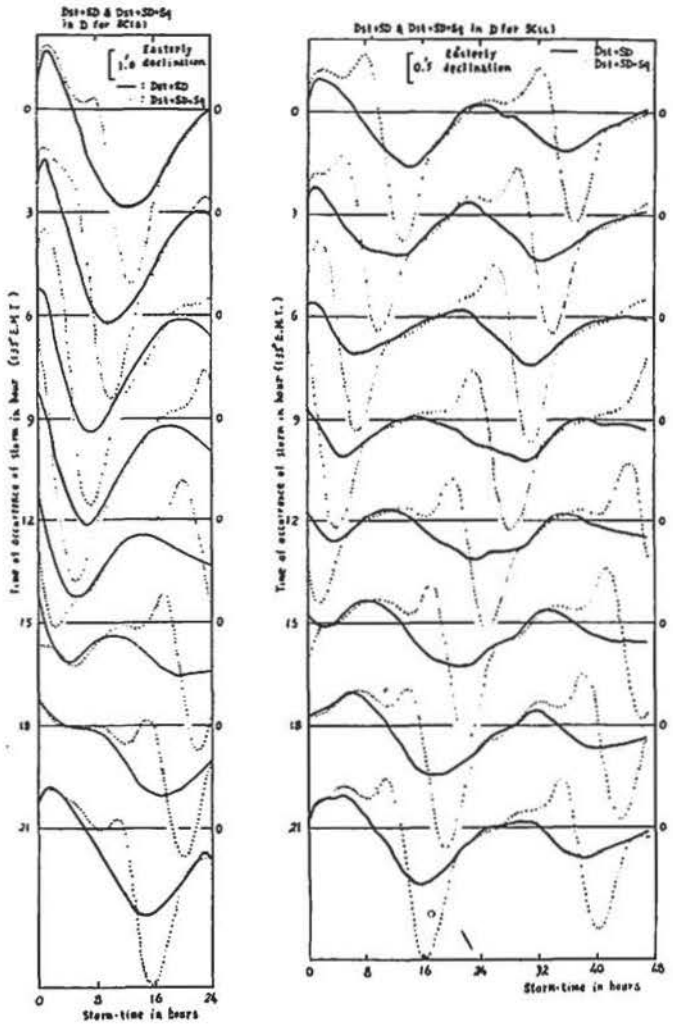

Fig. 21a. *Dst*+*SD* and *Dst*+*SD*+*Sq* of *ssc* commenced at different local times in D for storm group SC(a).

Fig. 21b. *Dst*+*SD* and *Dst*+*SD*+*Sq* of *ssc* commenced at different local times in D for storm group SC(c).

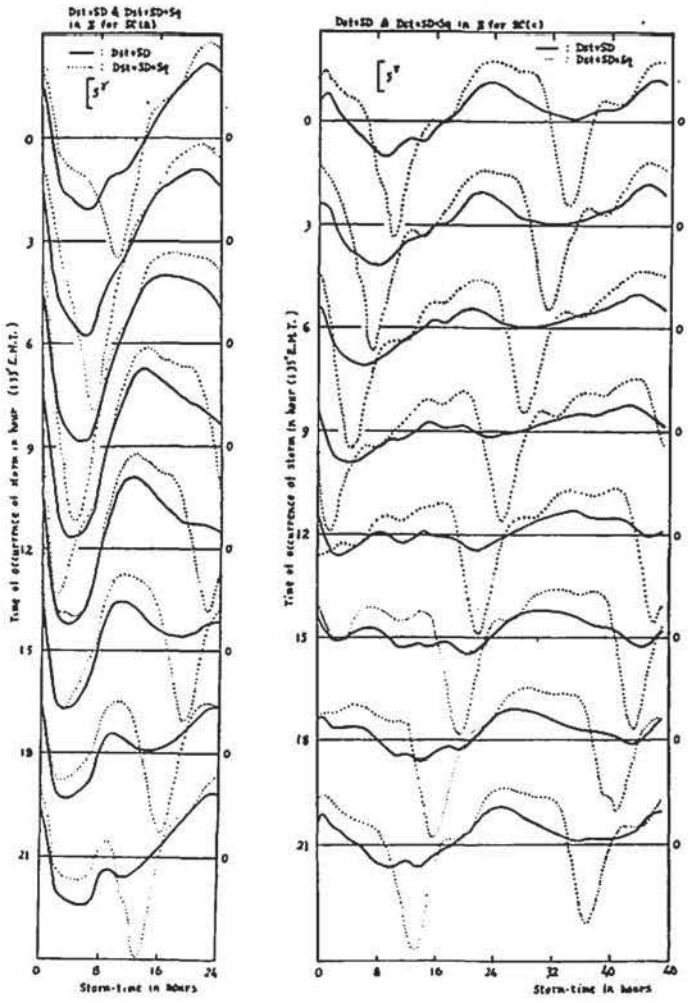

Fig. 22a. *Dst*+*SD* and *Dst*+*SD*+*Sq* of *ssc* commenced at different local times in Z for storm group SC(a).

Fig. 22b. *Dst*+*SD* and *Dst*+*SD*+*Sq* of *ssc* commenced at different local times in Z for storm group SC(c).

## § 4. Expected storm-local time diagrams of storms

In Fig. 14 are shown the smoothed curves for the harmonic amplitudes of *SD*-variations, and it is assumed for phases that for the diurnal component they are constant during all storm-times, namely, for H 0°, for D 75° or 60° and for Z 105°, and for the semi-diurnal component for H they are 300° at storm-time 0 hour, followed by the decrease of 30° every storm-time 1 hour. By the above data, the *SD*-variations are calculated for storms occurred at different local times and then sum of them and the mean *Dst* in the previous paper are obtained. In Fig. 15 are thus shown the expected *Dst*+*SD* variations and the observed values. From the figures it is seen that they are roughly resemble each other. In Fig. 16~19 are shown storm-local time diagrams introduced from the above expected *Dst*+*SD* variations. These are available to investigate the general feature of development of storm-field with storm-time, because irregularities are smoothed out. Fig. 19 show also the expected storm-local time diagrams which involve variations of the semi-diurnal component of *SD*. These diagrams are so resemble to the original diagrams, that it seems that these expected diagrams are fairly reliable.

## § 5. Expected *Dst*+*SD* and *Dst*+*SD*+*Sq* for storm occurred at different local times

In Fig. 20~22 are illustrated the expected *D*st+*SD* in solid line and the expectd *Dst*+*SD*+*Sq* in dotted line. This is available to inspect the observed record at Kakioka. In D and Z, variations of *Sq* are comparable to that of *Dst*+*SD* and so *Dst*+*SD* curves are greatly different from *Dst*+*SD*+*Sq* curves.

## Acknowledgement

The author wishes to express his hearty thanks to Dr. T. Yoshimatsu, Director of the Kakioka Magnetic Observatory, for his encouragement and valuable advice and to Dr. S. Imamiti, College of Science, Tokyo and Dr. N. Fukushima, Tokyo University for their valuable advices.

## References

(1) Yokouchi, Y. (1957) : Mem. Kakioka Mag. Obs., 8, 27-47
(2) Nagata, T. and H. Ono (1952) : Journ. Geomag. Geoelectr., 4, 108-113
(3) Sugiura, M. and S. Chapman (1957) : Geophysical Institute, Alaska, AF. 19(604)-1732